Linear stability of plane Poiseuille flow over a generalized Stokes layer

M. Quadrio, Fulvio Martinelli, Peter Schmid

Linear stability of plane Poiseuille flow over a generalized Stokes layer

Journal of Physics: Conference Series **318** (2011) 022033 doi:10.1088/1742-6596/318/2/022033

Linear stability of plane Poiseuille flow over a generalized Stokes layer

Maurizio Quadrio[1,2], Fulvio Martinelli[2] and Peter J Schmid[2]

[1] Dip. Ing. Aerospaziale, Politecnico di Milano, Campus Bovisa, I-20156 Milano
[2] Laboratoire d'Hydrodynamique (LadHyX), CNRS–École Polytechnique, F-91128 Palaiseau

E-mail: maurizio.quadrio@polimi.it

Abstract. Linear stability of plane Poiseuille flow subject to spanwise velocity forcing applied at the wall is studied. The forcing is stationary and sinusoidally distributed along the streamwise direction. The long-term aim of the study is to explore a possible relationship between the modification induced by the wall forcing to the stability characteristic of the unforced Poiseuille flow and the signifcant capabilities demonstrated by the same forcing in reducing turbulent friction drag. We present in this paper the statement of the mathematical problem, which is considerably more complex that the classic Orr–Sommerfeld–Squire approach, owing to the streamwise-varying boundary condition. We also report some preliminary results which, although not yet conclusive, describe the effects of the wall forcing on modal and non-modal characteristics of the flow stability.

1. Introduction

Friction drag is an important source of energy expense (i.e. waste) in extremely common and widespread applications like air (airplanes), ground (cars, trains) and marine (submarines, ships, freight carriers) transportation, as well as in the trasportation of liquids and gases through pipelines.

Several techniques are under active study worldwide by the research community to reduce turbulent friction drag. An extremely simple and convenient open-loop strategy to reduce turbulent drag with good energetic performance has been recently proposed by Quadrio *et al.* (2009). The basic idea consists in creating at the wall of a channel (pipe) flow a distribution of spanwise (azimuthal) velocity which varies in time and along the streamwise coordinate, to produce a wavelike wall forcing. Waves designed to reduce drag have been shown to decrease friction by more than 50%. Such a large benefit, moreover, comes at a small energetic cost, so that net energy saving of the order of more than 20% have been observed, and more is deemed to be possible once the technique is optimized for maximizing the net savings. The waves create a spanwise, unsteady and streamwise-modulated transversal boundary layer that has been named the generalized Stokes layer or GSL (Quadrio & Ricco, 2011). It is interesting to notice that near-optimal performances are guaranteed by stationary waves, where the spanwise wall forcing does not depen upon time and the GSL becomes stationary (SSL, as described by Viotti *et al.* (2009)). A complete review of this drag reduction technique is given by Quadrio (2011).

The present paper has thus turbulent skin-friction drag reduction as its background objective, but deals with a significantly different matter. We aim at exploring how the stability characteristics of the indefinite plane channel flow (Poiseuille flow) are modified by the presence of an additional component to the base flow given by the spanwise velocity distribution at the

wall. It is our hope that understanding how the GSL interacts with the Poiseuille flow in terms of linear stability properties will help understanding how the GSL affects the turbulent drag.

To begin with, we limit ourselves to the simpler case of standing waves (SSL) and describe in this paper the problem formulation that is required in this case where homogeneity in the streamwise direction is lost. We also report preliminary results that concern both modal and non-modal stability.

2. Problem statement

The governing equations are the incompressible Navier–Stokes equations written in cartesian coordinates for the geometry of an indefinite plane channel flow. Axes and velocity components are labeled as usual, with y indicating the wall-normal coordinate. At the wall the spanwise forcing is applied, and in the present paper, for simplicity sake, only a stationary forcing is considered. The wall boundary conditions are thus homogeneous for the u and v components, whereas the spanwise component is given by $w = A\cos(\kappa x)$ (stationary waves) on both the channel walls.

Throughout this paper, reference length and velocity scales are the channel half-gap h, and the centerline velocity U_P of the reference Poiseuille flow. The Reynolds numer ia consequently defined as $Re = U_P h/\nu$, where ν is the fluid viscosity.

2.1. The base flow

It has been shown by Quadrio & Ricco (2011) that, when the streamwise flow is laminar, its parabolic profile does not interact with the spanwise boundary layer (the SSL) created by the waves. The latter is a function of the coordinates x and y only.

The streamwise parabolic profile is simply given by the Poiseuille solution:

$$\overline{U}(y) = 1 - y^2 \tag{1}$$

The spanwise profile is given an analytic expression under the hypotheses that its thickness is small compared to the channel half-height, and the streamwise viscous diffusion term is negligible w.r.t. the wall-normal diffusion term. If the streamwise profile is linear within the SSL, with $u_{y,0}$ its slope at the wall, then the analytical solution is:

$$\overline{W}(x,y) = \frac{1}{\mathrm{Ai}(0)} \Re\left\{ \mathrm{e}^{j\kappa x} \mathrm{Ai}\left(-\frac{jy}{\delta_x} \mathrm{e}^{-j4/3\pi} \right) \right\}$$

with Ai indicating the Airy special function, and $\delta_x = (\nu/\kappa u_{y,0})$ expressing a representative wall-normal length scale of the transversal boundary layer, defined in terms of the fluid viscosity ν, the wave length $2\pi/\kappa$ of the wall forcing and the longitudinal wall shear $u_{y,0}$.

While this is probably the only possible approach (short of computing the base flow with DNS) in the turbulent case, in the laminar case where $\overline{U}$ is analytically known and given by Eq. (1), the spanwise base flow can be computed as follows.

Assuming invariance in spanwise direction one gets the following non-dimensional equation for the w velocity component:

$$\left(1 - y^2\right) \frac{\partial w}{\partial x} = \frac{1}{Re} \left(\frac{\partial^2 w}{\partial x^2} + \frac{\partial^2 w}{\partial y^2} \right)$$

The non-dimensional boundary condition is:

$$w(x, \pm 1, z, t) = \frac{A}{2} \left(\mathrm{e}^{j\kappa x} + \mathrm{e}^{-j\kappa x} \right)$$

As the equation is linear, has constant coefficients in x and periodic boundary condition, one uses separation of variables by assuming that:

$$w(x,y) = \frac{1}{2}\left(f(y)\mathrm{e}^{j\kappa x} + f^*(y)\mathrm{e}^{-j\kappa x}\right)$$

with $*$ denoting complex conjugate. By substitution one arrives at two (equivalent) equations for f and f^*. The one for f reads:

$$f'' - \kappa\left[\kappa + jRe\left(1-y^2\right)\right] f = 0$$

with $f(\pm 1) = A$. This equation can also be solved analytically using parabolic cylinder functions.

3. Equations for linear stability

Our interest here lies in studying the linear stability of such base flow to three-dimensional small disturbances. The usual procedure of converting the disturbance evolution equations into the well-known v-η formulation (Schmid & Henningson, 2001) leads in the present case to variable-coefficients equations. Our aim is thus to work around this problem, by first arriving to an extended form of the v-η formulation that accounts for the new base flow, and by then showing how they can still be Fourier-transformed in the streamwise direction, their variable coefficients notwithstanding.

We indicate with the capital letters $\overline{U} = \overline{U}(y)$ and $\overline{W} = \overline{W}(x,y)$ the base flow created respectively by the longitudinal pressure gradient $\overline{P}_x$ and by the spanwise alternating wall boundary condition, as described in the previous Section. The velocity field, sum of two-dimensional base flow and three-dimensional small perturbations, is then decomposed as:

$$U = \overline{U} + u \tag{2}$$

$$V = v \tag{3}$$

$$W = \overline{W} + w \tag{4}$$

After substitution into the Navier–Stokes equations, and after linearization via dropping the quadratic terms in the perturbation field, one obtains:

$$\begin{cases} u_x + v_y + w_z = 0 \\ u_t + \overline{U}u_x + v\overline{U}' + \overline{W}u_z = -\left(\overline{P}_x + p_x\right) + \dfrac{1}{Re}\overline{U}'' + \dfrac{1}{Re}\nabla^2 u \\ v_t + \overline{U}v_x + \overline{W}v_z = -p_y + \dfrac{1}{Re}\nabla^2 v \\ w_t + \overline{U}\ \overline{W}_x + \overline{U}w_x + u\overline{W}_x + v\overline{W}_y + \overline{W}w_z = -p_z + \dfrac{1}{Re}\left(\overline{W}_{xx} + \overline{W}_{yy}\right) + \dfrac{1}{Re}\nabla^2 w \end{cases}$$

In Quadrio & Ricco (2011) it is shown that the base flow components obey the following equations

$$\begin{cases} 0 = -\overline{P}_x + \dfrac{1}{Re}\overline{U}'' \\ \overline{U}\ \overline{W}_x = \dfrac{1}{Re}\left(\overline{W}_{xx} + \overline{W}_{yy}\right) \end{cases} \tag{5}$$

and thus the corresponding terms can be subtracted from the above perturbation equations. The final form in cartesian coordinates is then:

$$\begin{cases} u_x + v_y + w_z = 0 \\ u_t + \overline{U}u_x + v\overline{U}' + \overline{W}u_z = -p_x + \dfrac{1}{Re}\nabla^2 u \\ v_t + \overline{U}v_x + \overline{W}v_z = -p_y + \dfrac{1}{Re}\nabla^2 v \\ w_t + \overline{U}w_x + u\overline{W}_x + v\overline{W}_y + \overline{W}w_z = -p_z + \dfrac{1}{Re}\nabla^2 w \end{cases} \tag{6}$$

4. Wall-normal velocity-vorticity formulation

The usual procedure that in the case of plane Poiseuille flow leads to the Orr–Sommerfeld–Squire equations can still be applied here. There are two major differences, though; several additional terms arise due to the presence of $\overline{W}$, and the resulting two equations, which are now fully coupled, will not have constant coefficients, thus preventing the simple Fourier transform procedure leading to one-dimensional eigenvalue problems parametrized by the disturbance wavenumber.

4.1. Wall-normal vorticity equation

The wall-normal component of the vorticity vector is defined as

$$\eta = u_z - w_x$$

Its governing equation can be readily obtained by taking the x derivative of the z momentum equation, and subtracting it from the z derivative of the x momentum equation:

$$\eta_t + \left(\overline{U}\frac{\partial}{\partial x} + \overline{W}\frac{\partial}{\partial z}\right)\eta + \left(\overline{W}_x\frac{\partial}{\partial y} + \overline{U}'\frac{\partial}{\partial z} - \overline{W}_{xy} - \overline{W}_y\frac{\partial}{\partial x}\right)v - u\overline{W}_{xx} = \frac{1}{Re}\nabla^2\eta \qquad (7)$$

By comparing Eq. (7) with its counterpart in the Orr–Sommerfeld case, one notices, besides the additional terms containing the base flow $\overline{W}$, the appearance of one term containing the u velocity component. At this stage of the procedure, the system that relates u and w to (the first wall-normal derivative of) v and η is still a differential system, and cannot be conveniently used to get rid of this term via algebraic substitution.

4.2. Wall-normal velocity equation

The procedure to obatin an evolutive equation for v is analogous to that of the reference Orr-Sommerfeld case, and involves taking spatial derivatives of the momentum equations, as well as taking advantage of the continuity equation. It results in:

$$\begin{aligned}\frac{\partial}{\partial t}\nabla^2 v + \left(\overline{U}\frac{\partial}{\partial x} + \overline{W}\frac{\partial}{\partial z}\right)\nabla^2 v - \left(\overline{U}''\frac{\partial}{\partial x} + \overline{W}_{yy}\frac{\partial}{\partial z}\right)v \\ - 2\overline{W}_{xy}u_z - 2\overline{W}_x\frac{\partial}{\partial z}(u_y - v_x) + \overline{W}_{xx}v_z = \frac{1}{Re}\nabla^2\nabla^2 v\end{aligned} \qquad (8)$$

Analogously to what has been just observed for Eq. (7), the equation for v presents several additional terms compared to its Orr–Sommerfeld counterpart, among which some involve the velocity components u which, up to this stage, cannot be easily substituted.

4.3. Fourier transform in the spanwise direction

The governing equations present x-varying coefficients. A straightforward preliminary step is to apply a Fourier transform in the z direction, along which the coefficients are constants. We omit using different symbols for discriminating quantities which depend on z or on the spanwise wavenumber β. The operator Δ, used in the next two Equations, is defined as follows:

$$\Delta = \frac{\partial}{\partial x^2} + \frac{\partial}{\partial y^2} - \beta^2$$

and the dynamics of the system is described by the system:

$$\eta_t + \left(\overline{U}\frac{\partial}{\partial x} + j\beta\overline{W}\right)\eta + \left(\overline{W}_x\frac{\partial}{\partial y} + j\beta\overline{U}' - \overline{W}_{xy} - \overline{W}_y\frac{\partial}{\partial x}\right)v - u\overline{W}_{xx} = \frac{1}{Re}\Delta\eta \tag{9}$$

$$\begin{aligned}\frac{\partial}{\partial t}\Delta v + \left(\overline{U}\frac{\partial}{\partial x} + j\beta\overline{W}\right)\Delta v - \left(\overline{U}''\frac{\partial}{\partial x} + j\beta\overline{W}_{yy}\right)v \\ - 2j\beta\overline{W}_{xy}u - 2j\beta\overline{W}_x\left(u_y - v_x\right) + j\beta\overline{W}_{xx}v = \frac{1}{Re}\Delta\Delta v\end{aligned} \tag{10}$$

5. Fourier transform in the streamwise direction

That the (spanwise) base flow $\overline{W}$ has a sinusoidal dependence on x, and not just a generic one, is what is exploited to transform the perturbation equations in Fourier space, notwithstanding its variable coefficients. We first express the spanwise base flow as:

$$\overline{W}(x,y) = \Re\left[f(y)\mathrm{e}^{j\kappa x}\right] = \frac{1}{2}\left[f(y)\mathrm{e}^{j\kappa x} + f^*(y)\mathrm{e}^{-j\kappa x}\right]$$

so that the various derivatives of $\overline{W}$ become:

$$\begin{aligned}\overline{W}_x &= \frac{j\kappa}{2}\left[f(y)\mathrm{e}^{j\kappa x} - f^*(y)\mathrm{e}^{-j\kappa x}\right] \\ \overline{W}_{xx} &= -\kappa^2\overline{W} \\ \overline{W}_y &= \frac{1}{2}\left[f'(y)\mathrm{e}^{j\kappa x} + f^{*'}(y)\mathrm{e}^{-j\kappa x}\right] \\ \overline{W}_{yy} &= \frac{1}{2}\left[f''(y)\mathrm{e}^{j\kappa x} + f^{*''}(y)\mathrm{e}^{-j\kappa x}\right] \\ \overline{W}_{xy} &= \frac{j\kappa}{2}\left[f'(y)\mathrm{e}^{j\kappa x} - f^{*'}(y)\mathrm{e}^{-j\kappa x}\right]\end{aligned}$$

Now the above assumptions are inserted into Eqns. (9) and (10), and the unknowns are expanded as follows:

$$\eta(x,y,t;\beta) = \sum_{i=-M}^{+M}\hat{\eta}(y,t;\beta)\mathrm{e}^{ji\kappa x}$$

$$v(x,y,t;\beta) = \sum_{i=-M}^{+M}\hat{v}(y,t;\beta)\mathrm{e}^{ji\kappa x}$$

In the above expansions, i a positive integer that spans from $-M$ to M, with the truncation defined by M expressing the degree of spectral expansion of the flow variables and the bandwidth of the block-tridiagonal discretization matrices. $m \in [0,1)$ is a real number defining the actual expansion wavenumber $\alpha = (m+i)\kappa$ used in the following. With $m \neq 0$, we allow for a detuning of the perturbation against the base flow, and in particular $m = 1/2$ describes the case of subharmonic flow, while $m = 0$ implies that the perturbation is locked in to the fundamental wavenumber. The detuning wavenumber $m\kappa$ is a fraction of the base flow wavenumber κ, and the higher harmonics of the perturbations are spaced by κ.

The continuity equation and the definition of wall-normal vorticity are a differential system that relates v and η to u and w. This system can now be made algebraic if the above assumption is accounted for, so that:

$$\hat{u} = \frac{j}{\alpha^2 + \beta^2}\left(\alpha\frac{\partial\hat{v}}{\partial y} - \beta\hat{\eta}\right)$$

$$\hat{w} = \frac{j}{\alpha^2+\beta^2}\left(\alpha\hat{\eta} + \beta\frac{\partial\hat{v}}{\partial y}\right)$$

and this paves the way for arriving at the final form of the equations for v and η, described below.

5.1. Wall-normal vorticity equation
By introducing the operator $\hat{\Delta} = \partial^2/\partial y^2 - \alpha^2 - \beta^2$ Eq.(9) becomes:

$$\begin{aligned}
&\sum_{i\,=-M}^{+M}\left\{\frac{\partial\hat{\eta}}{\partial t} + j\alpha\overline{U}\hat{\eta} + j\beta\overline{U}'\hat{v} - \frac{1}{Re}\hat{\Delta}\eta\right\}\mathrm{e}^{j\alpha x} \\
&= \sum_{i=-M}^{+M}\left\{-\frac{j\beta}{2}\left[f(y)\mathrm{e}^{j\kappa x} + f^*(y)\mathrm{e}^{-j\kappa x}\right]\hat{\eta} - \frac{j\kappa}{2}\left[f(y)\mathrm{e}^{j\kappa x} - f^*(y)\mathrm{e}^{-j\kappa x}\right]\frac{\partial\hat{v}}{\partial y}\right. \\
&\qquad + \frac{j\kappa}{2}\left[f'(y)\mathrm{e}^{j\kappa x} - f^{*'}(y)\mathrm{e}^{-j\kappa x}\right]\hat{v} + \frac{1}{2}\left[f'(y)\mathrm{e}^{j\kappa x} + f^{*'}(y)\mathrm{e}^{-j\kappa x}\right]j\alpha\hat{v} \\
&\qquad\left. - \frac{\kappa^2}{2}\left[f(y)\mathrm{e}^{j\kappa x} + f^*(y)\mathrm{e}^{-j\kappa x}\right]\frac{j}{\alpha^2+\beta^2}\left(\alpha\frac{\partial\hat{v}}{\partial y} - \beta\hat{\eta}\right)\right\}\mathrm{e}^{j\alpha x}
\end{aligned} \tag{11}$$

Since the hatted variables depend on y and t (besides wall-parallel wavenumbers), and $f = f(y)$, in the above equation the dependence on the streamwise coordinate x is uniquely contained in the complex exponentials $\mathrm{e}^{j\alpha x}$ and $\mathrm{e}^{\pm j\kappa x}\mathrm{e}^{j\alpha x}$; as such, every term $q(x)$ of the equation can be Fourier-transformed according to the general formula

$$\hat{q}(\tilde{\alpha}) = \frac{\kappa}{2\pi}\int_0^{2\pi/\kappa} q(x)\mathrm{e}^{-j\tilde{\alpha}x}dx$$

When evaluating integrals of the kind

$$\int_0^{2\pi/\kappa}\mathrm{e}^{\pm j\kappa x}\mathrm{e}^{j\alpha x}\mathrm{e}^{-j\tilde{\alpha}x}dx$$

one exploits the orthogonality of the trigonometric functions to state that they are equal to $\delta_{\tilde{\alpha},\pm\kappa+\alpha}$ (Kronecker symbol), i.e. they are always zero unless $\alpha = \tilde{\alpha} - \kappa$. By introducing the further notation $\tilde{\Delta} = \partial^2/\partial y^2 - \tilde{\alpha}^2 - \beta^2$, Eq. (11) for a given $\tilde{\alpha}$ becomes:

$$\begin{aligned}
\frac{\partial}{\partial t}\hat{\eta}_{\tilde{\alpha}} = &-j\tilde{\alpha}\overline{U}\hat{\eta}_{\tilde{\alpha}} - j\beta\overline{U}'\hat{v}_{\tilde{\alpha}} + \frac{1}{Re}\tilde{\Delta}\hat{\eta}_{\tilde{\alpha}} \\
&- \frac{j\beta}{2}f\left(1 - \frac{\kappa^2}{(\tilde{\alpha}-\kappa)^2+\beta^2}\right)\hat{\eta}_{\tilde{\alpha}-\kappa} \\
&- \frac{j\beta}{2}f^*\left[1 - \frac{\kappa^2}{(\tilde{\alpha}+\kappa)^2+\beta^2}\right]\hat{\eta}_{\tilde{\alpha}+\kappa} \\
&- \frac{j}{2}\left[\kappa f\left(1 + \frac{\kappa(\tilde{\alpha}-\kappa)}{(\tilde{\alpha}-\kappa)^2+\beta^2}\right)\frac{\partial}{\partial y} - f'\tilde{\alpha}\right]\hat{v}_{\tilde{\alpha}-\kappa} \\
&+ \frac{j}{2}\left[\kappa f^*\left(1 - \frac{\kappa(\tilde{\alpha}+\kappa)}{(\tilde{\alpha}+\kappa)^2+\beta^2}\right)\frac{\partial}{\partial y} + f^{*'}\tilde{\alpha}\right]\hat{v}_{\tilde{\alpha}+\kappa}
\end{aligned} \tag{12}$$

5.2. Wall-normal velocity equation
An analogous derivation leads to the following form for the wall-normal velocity component:

$$\begin{aligned}
&\sum_{i=-M}^{+M}\left\{\frac{\partial}{\partial t}\hat{\Delta}\hat{v}+j\alpha\overline{U}\hat{\Delta}\hat{v}-j\alpha\overline{U}''\hat{v}-\frac{1}{Re}\hat{\Delta}\hat{\Delta}\hat{v}\right\}\mathrm{e}^{j\alpha x}\\
&=\sum_{i=-M}^{+M}\left\{-\frac{j\beta}{2}\left[f\mathrm{e}^{j\kappa x}+f^{*}\mathrm{e}^{-j\kappa x}\right]\hat{\Delta}\hat{v}+\frac{j\beta}{2}\left[f''\mathrm{e}^{j\kappa x}+f^{*''}\mathrm{e}^{-j\kappa x}\right]\hat{v}\right.\\
&\qquad\qquad-\beta\kappa\left[f'\mathrm{e}^{j\kappa x}-f^{*'}\mathrm{e}^{-j\kappa x}\right]\frac{j}{\alpha^2+\beta^2}\left(\alpha\frac{\partial\hat{v}}{\partial y}-\beta\hat{\eta}\right)\\
&\left.-\beta\kappa\left[f\mathrm{e}^{j\kappa x}-f^{*}\mathrm{e}^{-j\kappa x}\right]\left(\frac{j}{\alpha^2+\beta^2}\left(\alpha\frac{\partial^2\hat{v}}{\partial y^2}-\beta\frac{\partial\hat{\eta}}{\partial y}\right)-j\alpha\hat{v}\right)+\frac{j\beta}{2}\kappa^2\left[f\mathrm{e}^{j\kappa x}+f^{*}\mathrm{e}^{-j\kappa x}\right]\hat{v}\right\}\mathrm{e}^{j\alpha x}
\end{aligned}\tag{13}$$

After rearranging, and introducing the notation $\tilde{\Delta}_{\pm}=\partial^2/\partial y^2-(\tilde{\alpha}\pm\kappa)^2-\beta^2$ Eq. (13) can be rewritten as:

$$\begin{aligned}
\frac{\partial}{\partial t}\tilde{\Delta}\hat{v}_{\tilde{\alpha}}=&-j\tilde{\alpha}\overline{U}\tilde{\Delta}\hat{v}_{\tilde{\alpha}}+j\tilde{\alpha}\overline{U}''\hat{v}_{\tilde{\alpha}}+\frac{1}{Re}\tilde{\Delta}\tilde{\Delta}\hat{v}_{\tilde{\alpha}}\\
&+\frac{j\beta^2\kappa}{(\tilde{\alpha}-\kappa)^2+\beta^2}\left(f'+f\frac{\partial}{\partial y}\right)\hat{\eta}_{\tilde{\alpha}-\kappa}\\
&-\frac{j\beta^2\kappa}{(\tilde{\alpha}+\kappa)^2+\beta^2}\left(f^{*'}+f^{*}\frac{\partial}{\partial y}\right)\hat{\eta}_{\tilde{\alpha}+\kappa}\\
&-\frac{j\beta}{2}\left[f\tilde{\Delta}_{-}-f''-\kappa f\left(2\tilde{\alpha}-\kappa\right)+2\frac{\kappa(\tilde{\alpha}-\kappa)}{(\tilde{\alpha}-\kappa)^2+\beta^2}\left(f'\frac{\partial}{\partial y}+f\frac{\partial^2}{\partial y^2}\right)\right]\hat{v}_{\tilde{\alpha}-\kappa}\\
&-\frac{j\beta}{2}\left[f^{*}\tilde{\Delta}_{+}-f^{*''}+\kappa f^{*}\left(2\tilde{\alpha}+\kappa\right)-2\frac{\kappa(\tilde{\alpha}+\kappa)}{(\tilde{\alpha}+\kappa)^2+\beta^2}\left(f^{*'}\frac{\partial}{\partial y}+f^{*}\frac{\partial^2}{\partial y^2}\right)\right]\hat{v}_{\tilde{\alpha}+\kappa}
\end{aligned}\tag{14}$$

6. Results

We present in this Section a few representative and preliminary results that have been obtained so far. The present study is essentially a parametric study that requires exploring a huge parameter space, where the following physical parameters are at play: Re, A, κ, β. In addition, there are two discretization parameters N and M. The former follows from the discretization of the wall-normal direction, where we use a number N of Chebishev polynomials. Besides, and peculiar to the present study, the truncation of sums (12) and (14) highlights the further, crucially important parameter M. It quantifies how far in the modal space we allow the interaction between different harmonics to take place. For a given value of Re, A, κ, and β, the computational problem is that of computing eigenvalues of a large matrix, its size being comparable to that of a standard Orr-Sommerfeld problem multiplied by a factor $(2M+1)^2$. Typical values of M are around $20-50$, and thus special care is required to keep the computational load down to a reasonable level.

The preliminary results discussed in the following have been obtained with discretization parameters good enough to ensure their reliability. However, the span of the parameter space is far from complete yet. Moreover, only the value $m=0$ for the detuning parameter is considered: no subharmonics are allowed.

6.1. Validation

As a first step, validation against a DNS code is carried out for the following conditions: $Re = 9000$, $A = 1$, $\kappa = 1$. For the calculation of the most unstable eigenvalue in the stability code, we employ $N = 90$ Chebishev polynomials and $M = 9$. The DNS is carried out with the same DNS code employed by Quadrio *et al.* (2009). The predicted growth rate from the linear stability code is 0.00898 for the dominant mode, and twice that for the growth of its energy. Figure 1 is a nice validation of the stability code. DNS is inizialized with small-amplitude random noise, and clearly shows after a transient period the emergence of a dominant mode whose energy grows at exactly the expected rate.

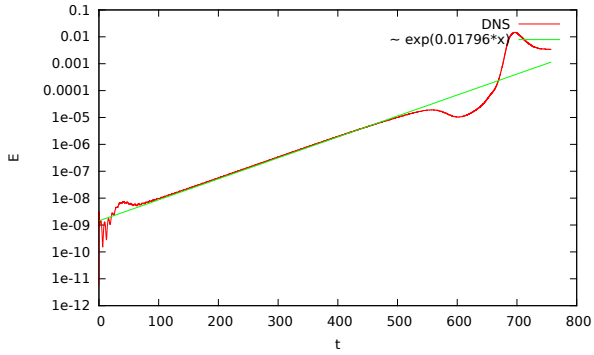

Figure 1. Validation of the calculation of the most unstable eigenvalue. Green straight line is energy growth prediction from the linear stability code, whereas red line is the DNS-computed temporal evolution of perturbation energy.

6.2. Modal stability

Results are only available at one value of the Reynold number, namely $Re = 2000$. We show in figure 2 how the main parameters affect the growth rate of the least stable perturbation, as deduced by the eigenvalue with the largest real part.

6.3. Nonmodal stability

The search for the eigenvalue with the largest real part implies the assumption that perturbations have an exponential time dependence (decay or growth). This is also referred to as the modal or normal-mode approach. The limitations of this assumptions for non-normal systems like the present one, where the system matrix possesses a set of non-orthogonal eigenvectors, are

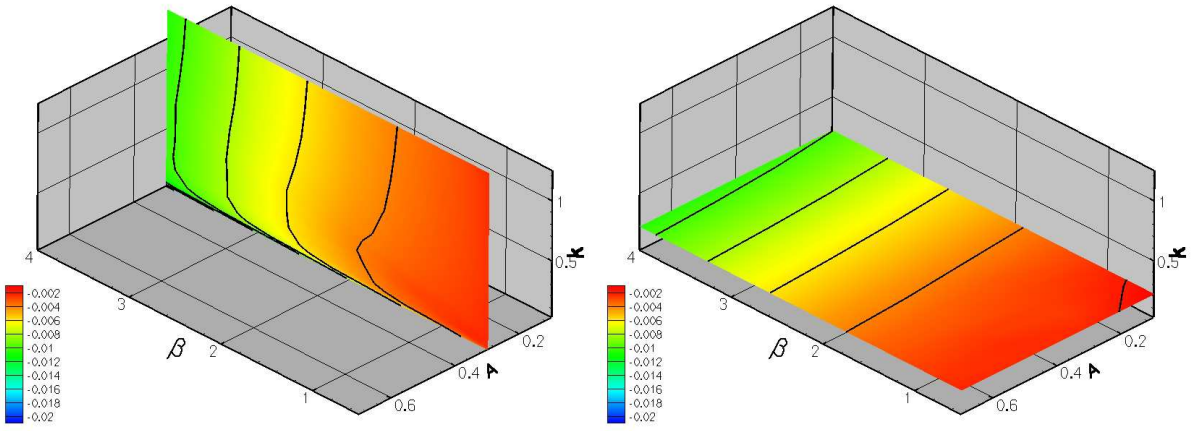

Figure 2. Maximum growth rate at $Re = 2000$, as a function of the parameters κ, A and β.

nowadays well known. This is why we additionally provide here for the system at hand a study of nonmodal stability characteristics, which focus on the short-time behaviour of the perturbation.

Following the general theory (Schmid, 2007), an energy norm has to be defined first as the proper measure of the disturbance size. In the present case, the physically sound definition in terms of kinetic energy is adopted. After translating this definition into the $v-\eta$ formulation, it is easy to write an expression for the energy density $E(\alpha,\beta)$, and express it in matrix form. It is then possible to compute the growth function $G(t)$, defined as the transient growth of the energy of the initial condition, maximized over all possible initial conditions:

$$G(t) = \max_{\mathbf{x}_0} \frac{\| \mathbf{x}(t) \|_E^2}{\| \mathbf{x}_0 \|_E^2}$$

where $\mathbf{x}(t)$ is the system state vector, $\mathbf{x}_0$ the initial state, and the index E indicates an energy norm. An example of the transient growth of perturbation energy is shown in figure 3 for one case at $Re = 1000$, $A = 0.65$, $\kappa = 0.5$ and $\beta = 1.5$. The employed discretization is $N = 90$ and $M = 16$.

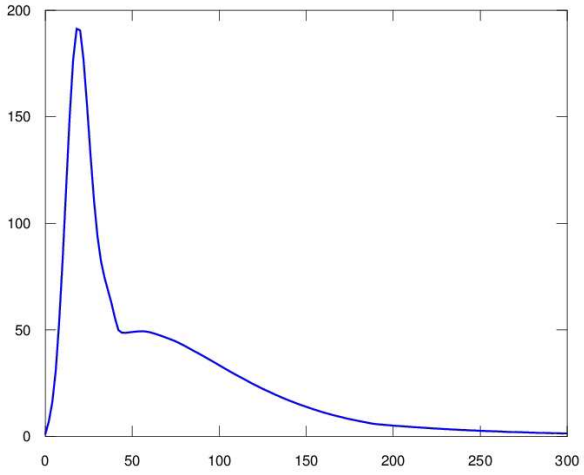

Figure 3. Transient growth of perturbation energy for $Re = 1000$, $A = 0.65$, $\kappa = 0.5$, $\beta = 1.5$.

A non-modal analysis provides us also with the spatial shape of the optimal input, or optimal initial condition, i.e. that spatial shape of the pertubation at $t = 0$ that is capable of maximum amplification before long-term decay. In the present problem, the optimal initial condition is not constrained to be described by a single streamwise wave-number, and looking at it in the $i-y$ plane is useful to assess the spatial resolution employed (N) as well as the width of harmonic interplay (M). Figure 4 concerns the same calculations just described above, and plots the modulus of the inital condition in terms of wall-normal velocity (left) and wall-normal vorticity (right) as a function of the wall-distance, and of the index i of the modal expansion. It can be appreciated how the amplitude of the initial condition is distributed along the channel gap, but – most important – this figure demonstrates that M has been chosen large enough, since the spectral energy shows compact support in this representation.

7. Conclusions

We have studied the linear stability of plane Poiseuille flow modified by a wall velocity forcing in the form of streamwise stationary waves of spanwise velocity. Both modal and non-modal stability characteristics have been addressed.

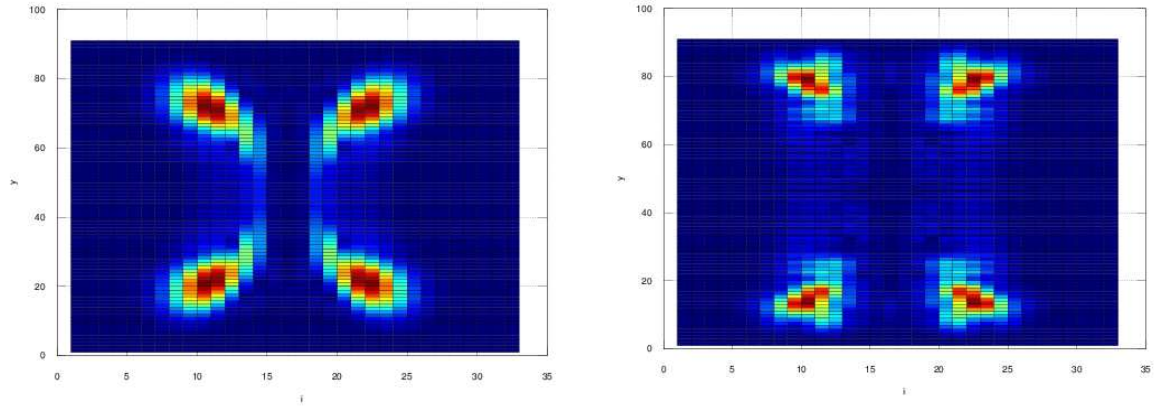

Figure 4. Optimal initial condition for the wall-normal velocity (left) and wall-normal vorticity (right) as a function of the wall-normal position y and the index i of the modal expansions (12) and (14). The color scale describes the modulus of the inital condition.

The mathematical formulation of the problem, and its numerical implementation, are not straightforward, the main reason being that the wall forcing introduces a streamwise inhomogeneity that prevents exploiting a simple transform in Fourier space to decouple it into a one-dimensional eigenvalue study parametrized on the perturbation wavenumber. After writing the equations in the wall-normal velocity and wall-normal vorticity form, the sinusoidal variation of the spanwise baseflow is exploited to obtain a formulation amenable to an affordable numerical solution. The preliminary results shown here are the starting point for a full study that must span the entire parameter space to understand how this form of spanwise forcing affects the stability of plane Poiseuille flow.

Acknowledgments

This work has been carried out while MQ was spending a sabbatical leave at LadHyX. The kind hospitality and economic support provided by the host lab is gratefully acknowledged.

References

Quadrio, M. 2011 Drag reduction in turbulent boundary layers by in-plane wall motion. *Phil. Trans. R. Soc. A* **369** (1940), 1428–1442.

Quadrio, M. & Ricco, P. 2011 The laminar generalized Stokes layer and turbulent drag reduction. *J. Fluid Mech.* **667**, 135–157.

Quadrio, M., Ricco, P. & Viotti, C. 2009 Streamwise-traveling waves of spanwise wall velocity for turbulent drag reduction. *J. Fluid Mech.* **627**, 161–178.

Schmid, P. 2007 Nonmodal stability theory. *Annu. Rev. Fluid Mech.* **39**, 129–162.

Schmid, P.J. & Henningson, D.S. 2001 *Stability and Transition in Shear Flows*. Springer.

Viotti, C., Quadrio, M. & Luchini, P. 2009 Streamwise oscillation of spanwise velocity at the wall of a channel for turbulent drag reduction. *Phys. Fluids* **21**, 115109.